Factors Limiting the Upper Frequency of mm-Wave Spherical Near-field Test Systems

Daniël Janse van Rensburg[1]
[1] Nearfield Systems Inc, 19730 Magellan Drive, Torrance, CA 90502-1104, USA
e-mail: drensburg@nearfield.com

***Abstract* — Antennas operating at mm-wave frequencies have led to the development of spherical near-field test systems that have to function at higher frequencies than before. This paper addresses some of the factors limiting the upper frequency bound of spherical near-field test systems in terms of what is practical with current technology. This includes mechanical positioning systems, RF sub-systems and the spherical near-field sampling requirements. Correction techniques that have been developed to enhance the performance of such measurement systems are also presented.**

***Index Terms*— *S*pherical near-field, mm-wave, antenna measurement.**

I. INTRODUCTION

When considering antenna measurements at mm-wave and sub-mm-wave frequencies, planar near-field systems have become commonplace [1, 2, 3]. In this process most of the RF and mechanical challenges were successfully identified and addressed [4, 5, 6]. However, planar near-field systems are limited to measuring higher gain antennas and as the number and variety of test applications at these high frequencies have increased, so too has the need for spherical near-field (SNF) test systems. One such a system using precision positioners that meet the stringent alignment requirements imposed by the spherical geometry, was described in [7]. A second unique system that does not require any motion of the antenna under test was described in [8]. In [9] an articulated arm design which transports a probe over a hyper-hemispherical surface in front of the antenna was presented. In the latter publication results of a parametric study that was undertaken to investigate the viability of that system, was presented. Parameters such as probe radial distance and angular positioning uncertainty were investigated to assess to what extent high frequency SNF testing could be performed using commercially available positioners.

In this paper measured results are presented that were acquired on a SNF scanner like that described in [9] and depicted in Fig. 1 below. Measured laser tracker coordinate information is also presented here and the radial correction technique proposed during the earlier design phase is evaluated.

An assessment of using this type of test system for SNF testing is given and an optional approach of using this type of system for simple far-field testing is also described.

II. ARTICULATED SPHERICAL NEAR-FIELD ANTENNA TEST SYSTEM

The SNF antenna test system of interest here is as illustrated and depicted in Fig. 1.

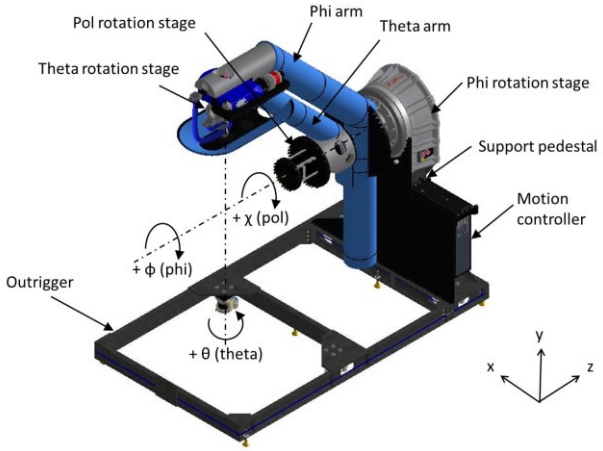

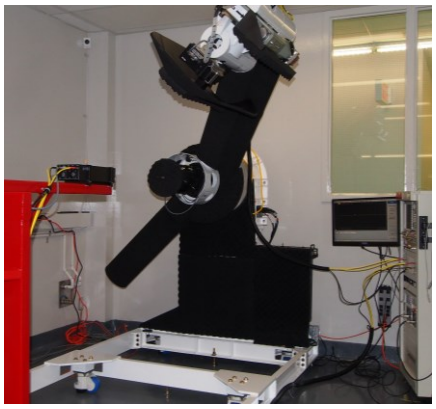

Fig. 1. Schematic representation and actual NSI-700S-360 articulated spherical near-field antenna test system showing the associated spherical measurement coordinate system.

This consists of a 500 mm positioner mounted on a large floor stand. This positioner defines the horizontal ϕ-axis of rotation and this coincides with the z-axis of the measurement coordinate system. A second rotary stage is attached to this stage at an angle of 90° to the ϕ-axis and this second stage forms the θ-axis of a conventional right handed polar spherical

coordinate system. A third rotary stage is attached to the θ-stage at an angle of 90° to the θ-axis and this third stage forms the χ-axis. The combined motion of the ϕ and θ stages allows the probe tip to describe the trajectories located on a spherical surface centred about the intersection of those orthogonal axes and whose definition is in accordance with standard SNF theory [10]. Crucially, and as is the case for planar measurements, data is acquired across a two-dimensional sampling interval with the antenna under test (AUT) remaining entirely at rest (a feature of particular interest when measuring on-chip antennas).

III. Scanner Stuctural Data

Scanner structural and positioning performance data can be obtained from laser tracker dimensional measurements. These results allow one to establish a perturbed (θ′, ϕ′, *r*′) grid, based on a regular (θ, ϕ, *r*) SNF grid. For the scanner shown in Fig.1 the total region of motion is depicted in Fig. 2 and this spans a surface limited by -110° ≤ θ ≤ 110° and 0 ≤ ϕ ≤ 180°. It should be noted that these limitations are determined by the requirement to locate an RF rack and AUT support in the keep-out region. Results obtained for *r*′ as a function of (θ, ϕ) are depicted below in Fig. 3 in the form of a false colour checkerboard plot. Radial distance variation measured was ±1.6 mm and angular location variation (not shown) was ±0.2° peak-to-peak for both θ′ and ϕ′.

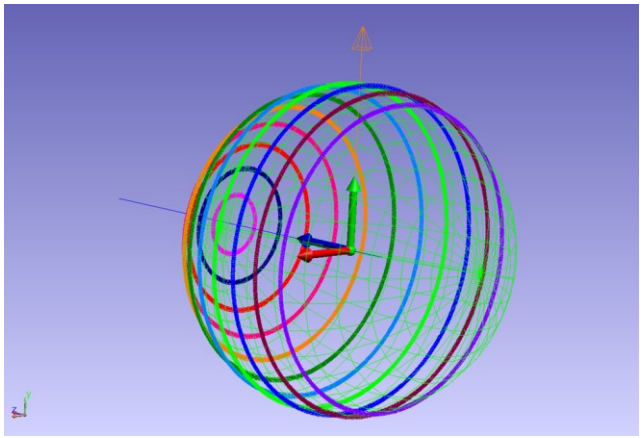

Fig. 2. *NSI-700S-360 Articulating SNF scanner probe tip trajectory & coordinate system. Axes are: z-axis (blue, horizontal and pointing at N-pole), y-axis (green, vertical), x-axis (red, horizontal).*

Based on the result of the measurement radius r′ a corresponding electrical phase correction pattern can be generated at each frequency of interest. This phase correction can then be applied to the measured SNF data as a first order correction term in an attempt to remove the phase impact of the structural variation. This correction is referred to as R-correction below. Although a similar correction can be considered for angular uncertainties, that was not implemented here as these are typically found to be secondary in nature.

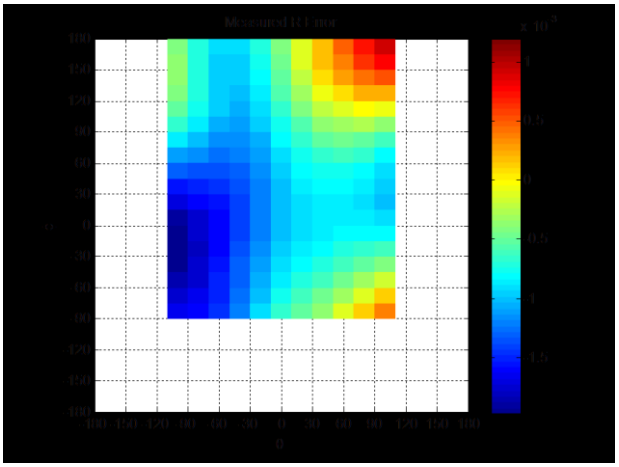

Fig. 3. *Scanner radius r′ shown as a function of (θ, ϕ). The radius variation observed is ±1.6 mm.*

IV. Measured Data

During testing the horn antenna shown in Fig. 4 below was measured in the 90 – 110 GHz band. At the upper end of this band the radial uncertainty of ±1.6 mm translates to ± 211° of electrical phase and this does not include any impact of the RF guided wave path. Two measurements were therefore made, a first reference measurement of the principal plane cuts which was made in the far-field and a second SNF measurement, taken over a full hemisphere at the required sampling density.

Fig. 4. *Antenna under test, operational in the 90 – 110 GHz band.*

The corresponding far-field results are depicted below in Fig. 5 (90 GHz at the top and 110 GHz at the bottom). The reference far-field patterns are shown as the solid line and the finite signal to noise ratio of the mm-wave RF sub-system is evident. As expected, the SNF measurement is significantly affected by the phase error induced by the radial probe positioning uncertainty and the short dashed pattern depicts this result (legend - R corr off). Once the radial distance phase correction is applied to the near-field data a new corrected far-field pattern can be extracted and this is depicted below as the long dashed pattern (legend - R corr on). The corrective impact of the reprocessed result is evident and was also extracted for orthogonal plane radiation patterns (not shown here). These results illustrate how a laser tracker structural measurement can be introduced to enhance the ability of such scanners for use at higher frequencies. The obvious requirement in this instance is that the structure motion be repeatable since the correction technique will not be effective otherwise.

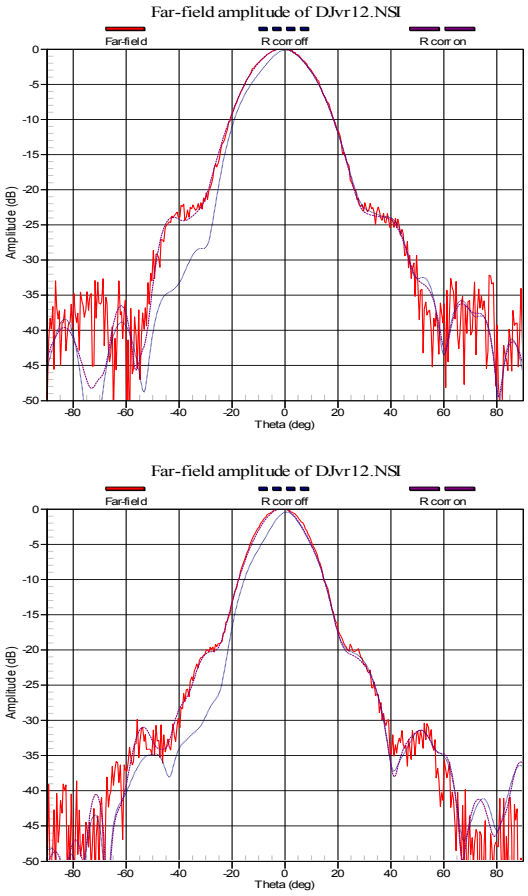

Fig. 5. *Far-field reference pattern (solid) is shown overlaid with SNF derived far-field patterns for cases where no radial phase correction is applied (--) and where radial phase correction IS applied (- -). Result at 90 GHz is shown at the top and 110 GHz at the bottom.*

V. NEAR-FIELD VS. FAR-FIELD ASSESSMENT

SNF testing requires the acquisition of discrete field samples on a spherical surface. The number of samples is determined by the electrical size of the antenna under test and the specific mounting thereof, allowing for a minimum radius sphere (*MRS*) to be defined [10]. The maximum number of spherical modes is denoted by N and is related to the *MRS* through

$$N = \frac{2\pi MRS}{\lambda} + 10$$

If we now set the *MRS* equal to a radius a we can write the following expression that relates antenna directivity (*Dir*) to N

$$N = \sqrt{\frac{Dir}{\eta}} + 10$$

where *Dir* is the aperture directivity (linear) and η is the aperture efficiency which are related to the aperture area A (or πa^2 for a circular aperture) by

$$Dir = \frac{4\pi\eta A}{\lambda^2} = \frac{4\pi^2 \eta a^2}{\lambda^2}$$

The significance of the relationship between N and *Dir* is that for an antenna of fixed directivity, the number of representative spherical modes remains constant, regardless of frequency. Since the antenna remains of constant electrical size, it is shrinking in physical size as a function of increasing frequency but angular sampling density when measured on a SNF range remains fixed since the *MRS* in terms of wavelength remains constant. The table below shows some typical directivity values in dB and the associated number of SNF modes that would be required to characterize those antennas, assuming an aperture efficiency of 50%.

Dir [dB]	Dir	N
5	3.2	13
10	10.0	14
15	31.6	18
20	100.0	24
30	1000.0	55
40	10000.0	151
50	100000.0	457

Table 1: Spherical mode index tabulated against antenna directivity.

Since the value of N is directly proportional to the SNF sampling density, we can now use the peak-to-peak angular positioning uncertainty value of ±0.2° to set our expected minimum sampling interval to 2°, which would correspond to N = 90. (In [7] it was shown that a random error of less than 1/10 of the sampling interval is required to achieve far-field error levels of < –30 dB.) This sampling interval can now be converted to a maximum *Dir* value of roughly 35 dBi.

It is important to state that SNF testing at mm-wave frequencies is driven by antenna electrical size and not by frequency. We can therefore conclude that the maximum angular positioning uncertainty during SNF testing is driven by the angular sampling interval and not by the frequency or wavelength of operation. For the scanner being considered here we can therefore state that the largest electrical size of an antenna that can be measured in SNF mode is one that corresponds to a directivity value of 35 dBi and if the radial position of the probe was perfect, there would be no upper frequency limit. However, since there is radial positioning uncertainty and RF cable flexing will limit the extent to which this could be corrected for, a practical upper limit for SNF testing is probably in the range of 110 GHz.

Since SNF measurements require phase to be measured, a convenient alternative is to consider far-field testing (amplitude only). Here it is worthwhile to consider the familiar far-field criterion expressed in terms of antenna directivity

$$R = \frac{2D^2}{\lambda} = \frac{2\lambda Dir}{\eta\pi^2}$$

where R is the required far-field distance and D is the largest dimension of the radiating aperture (assuming that the AUT is located at the origin of the measurement coordinate system). This expression for the far-field distance R is significant in that it shows that for an antenna of specific directivity, the far-field distance for testing reduces as a function of increasing frequency (therefore a different behavior from what one observes for SNF angular sampling density); A simple (though not intuitive) result. A result of this observation is that we can specify a far-field test system with say a 500 mm distance R, that allows us to write

$$\frac{\pi^2}{4} = \frac{\lambda D i r}{\eta}$$

This simple expression now allows one to evaluate the maximum directivity value of an antenna that can be tested on a 500 mm far-field antenna range as a function of frequency. This is shown below in Fig. 6.

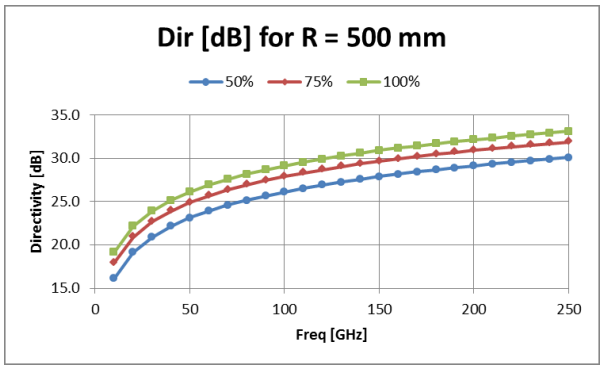

Fig. 6. Maximum antenna directivity that can be tested in the far-field mode at a 500 mm distance. Directivity shown in dB as a function of frequency for 50%, 75% and 100% aperture efficiency.

The result shown in Fig. 6 is for η = 50%, 75% and 100% aperture efficiency and it is significant in that it shows that for a fairly moderate fixed far-field distance of 500 mm, higher gain antennas can readily be measured in the far-field as the frequency is increased.

If we now consider the single test system as described and characterized here, we can state that the system will allow for testing of antennas of up to directivity values of 35 dBi in SNF mode, up to a maximum frequency of roughly 110 GHz. Beyond that frequency antennas of maximum directivity of roughly 26 dBi can be measured as depicted in Fig. 6. The system can of course also be used for far-field testing at lower frequencies, given lower directivity values as shown.

VI. Conclusions

The data presented here are for an articulated arm SNF scanner that was designed and built for mm-Wave testing. The positioning system was assessed using a laser tracker dimensional measurement system that characterized the system in terms of structural deflection during operation. This gravitationally induced structural deformation affects radial distance and angular positioning and this information was subsequently used to generate corrected measured data sets for an antenna operational in the 90 – 110 GHz band.

The results presented show a high sensitivity to probe radial distance variation, as was predicted during design [9]. First order correction for radial distance variation was performed by counter adjustment of the phase value of each measured tangential electric field component data point in the SNF data set and this proved to be a successful compensation strategy. Comparison to far-field measured data shows this clearly. This fact again emphasizes that this type of test system may be rendered of limited use at mm-Wave frequencies, unless this type of correction is performed.

No angular positioning correction was made during the SNF testing performed here since radial position correction proved to be the more challenging and critical concern.

The limits of operation for this test system are given in terms of maximum antenna directivity and frequency that can be tested in SNF mode and a simple relationship that shows the maximum antenna directivity that can be measured in far-field mode, given the fixed radial distance of 500 mm.

References

[1] D. Slater, “A 550 Ghz Near-Field Antenna Measurement System for The NASA Submillimeter Wave Astronomy Satellite”, Antenna Measurement Techniques Association Conference, October 3-7, 1994.

[2] D. Slater, P. Stek, R. Cofield, R. Dengler, J. Hardy, Robert Jarnot, Ray Swindlehurst, “A Large Aperture 650 GHz Near-Field Measurement System for the Earth Observing System Microwave Limb Sounder”, Antenna Measurement Techniques Association Conference, 2001.

[3] P.W. Bond, G.A. Ediss, “Design, Alignment, and Calibration Requirements for a Submillimeter Wave Frequency Tiltable Lightweight Scanner”, Antenna Measurement Techniques Association Conference, 2007.

[4] D. Janse van Rensburg, “A Technique To Evaluate The Impact of Flex Cable Phase Instability on mm-Wave Planar Near-Field Measurement Accuracies”, ESA ESTEC

[5] D. Janse van Rensburg, “Compensation for Probe Translation Effects in Dual Polarized Planar Near-Field Antenna Measurements”, Antenna Measurement Techniques Association Conference, 2008.

[6] D. Janse van Rensburg, G.E. Hindman, “An Overview of Near-Field Sub-millimeter Wave Antenna Test Applications”, COMITE Conference, Czech Republic, 23-24 April, 2008.

[7] D. Janse van Rensburg, J. Wynne, “Parametric Study of Probe Positioning Errors in Spherical Near-field Test Systems for mm-Wave Applications”, IEEE APS/URSI, Conference Chicago, 2012.

[8] G.E. Hindman, H. Tyler, “High Accuracy Spherical Near-Field Measurements on a Stationary Antenna”, Antenna Measurement Techniques Association Conference, 2010.

[9] D. Janse van Rensburg and S. Gregson, “Parametric Study of Probe Positioning Errors in Articulated Spherical Near-field Test Systems for mm-Wave Applications”, IEEE Conference on Antenna Measurements & Applications, Antibes Juan-les-Pins (France), 16-19th Nov. 2014.

[10] C. Parini, S. Gregson, J. McCormick & D. Janse van Rensburg, *Theory and Practice of Modern Antenna Range Measurements*, IET, London, 2014. ISBN 978-1-84919-560-7